RSC Advances

PAPER

View Article Online
View Journal | View Issue

Cite this: *RSC Adv.*, 2025, **15**, 34595

Efficient preparation of highly fluorescent dual-emission carbon dots and their application in berberine hydrochloride detection

Yang Geng, *[a] Ze-Yue Zhao,[a] Wei Zhang,[a] Long-Teng Li,[a] Ye Tian,[a] Bai-Qiang Zhai,[a] Wen-Zhu Bi, [b] Wen-Jie Zhang*[b] and Yang-Guang Wang*[c]

In this study, dual-emission fluorescent carbon dots (DE-CDs) with high fluorescence quantum yield (46%) were efficiently prepared through a one-step hydrothermal strategy using L-arginine and 1-pyrenecarboxaldehyde as precursors. The hydrothermal reaction conditions were optimized, and the morphological structure and elemental composition were characterized. The investigation of optical properties showed that the as-prepared DE-CDs displayed two maximum emissions at 378 and 398 nm upon excitation at 340 nm with superior photobleaching resistance, thermostability, pH stability and salt tolerance. In addition, the two fluorescence emissions could be selectively quenched by berberine hydrochloride (BH) with good linear correlation (R^2 = 0.9970 and 0.9967) in the range of 0–10 μM. Therefore, a fluorescence detection platform for BH was developed with low detection limits (0.32 and 0.30 μM), short response time (<10 s) as well as good recoveries for actual samples (92–110%). Finally, the quenching mechanism was studied and proposed to be a combination of the inner-filter effect (IFE, 62.66%) and fluorescence resonance energy transfer (FRET).

Received 5th August 2025
Accepted 9th September 2025

DOI: 10.1039/d5ra05692f

rsc.li/rsc-advances

Introduction

Berberine is a quaternary isoquinoline-based alkaloid that naturally occurs in traditional Chinese medicine, such as coptis, cypress and goldenseal. It is also known as *Coptis rhizome* and is typically used in the form of berberine hydrochloride (BH). Numerous studies have shown that BH displays tremendous therapeutic potential,[1] including for the treatment of hypertension[2] and obesity,[3] pain relief,[4] liver protection[5] and anticancer activity.[6,7] Due to its bioactivity and wide applications, the development of sensitive and rapid detection methods for BH is particularly important in the quality evaluation of traditional Chinese medicine and in pharmaceutical analysis. The conventionally used detection methods are redox titration and high-performance liquid chromatography (HPLC).[8] However, these methods suffer from complicated and time-consuming detection processes as well as expensive instruments. In order to realize sensitive and convenient detection of BH, new detection strategies, such as capillary electrophoresis,[9] electrochemical analysis,[10] photoelectrochemical[11] and metal nanoparticle-based chemiluminescence[12] methods, have been rapidly developed in recent years. Although these strategies have the advantages of good selectivity and sensitivity, they still have the disadvantages of complex preparation processes[9–11] and employment of noble or heavy metals (*e.g.* Ag, Au, and Cu).[12] Therefore, it is of great significance to establish a rapid, simple and low-cost method for the quantitative analysis of BH.

To address this issue, carbon dot (CD)-based fluorescence methods stand out due to their low-cost and simple preparation, excellent photoluminescence as well as good selectivity and sensitivity.[13] Similar probes were developed for BH detection by Yan *et al.*, Ren *et al.* and Tan *et al.* in 2021 and 2022.[14] However, all the CDs employed in these methods exhibited single-fluorescence emission and were easily affected by the concentration and uniformity of sensors, environmental conditions and instrument status.[15] Comparatively, dual-emission fluorescent CDs can overcome these disadvantages and improve the sensitivity and accuracy by simultaneously monitoring two fluorescence intensities.[16] Therefore, dual-emission CDs have developed very rapidly in the fields of pharmaceutical analysis, environmental monitoring and bioimaging.[17] However, despite the great achievements made on the applications of CDs, the pursuit of CDs with efficient preparation method, simple synthetic precursors, high quantum yield and excellent optical properties never ends.

Based on the above considerations and our previous works relating to the facile synthesis and application of novel CDs,[18] we would like to demonstrate here an efficient preparation of

[a]*Department of Pharmacy, Zhengzhou Railway Vocational and Technical College, Zhengzhou, 451460, China. E-mail: gengyang5323@163.com*
[b]*School of Pharmacy, Henan University of Chinese Medicine, Zhengzhou, 450046, China. E-mail: zwj9007@163.com*
[c]*Triz Pharmaceutical, Zhengzhou Triz Pharmaceutical Technology Co., Ltd, Zhengzhou, 450000, China. E-mail: wangyangguang@trizpharma.cn*

dual-emission CDs (DE-CDs) using easily available L-arginine and 1-pyrenecarboxaldehyde as precursors through a one-step hydrothermal method at 190 °C for 4 h, as shown in Scheme 1. The morphological structure and elemental compositions were carefully characterized and indicated the successful synthesis of carbon dots. The dual blue fluorescence emission at 378 and 398 nm of DE-CDs showed superior photobleaching resistance, thermostability, pH stability and salt tolerance with relatively high fluorescence quantum yield (FLQY: 46%). Importantly, the two emission peaks could be instantly quenched by BH with good linearity and a low detection limit over the range of 0–10 μM. Furthermore, the detection of BH in actual samples (berberine hydrochloride tablets and capsules) showed good recoveries with relative standard deviations (RSD) less than 5%. Finally, the quenching mechanism was proposed to be a combination of the inner-filter effect (IFE) and fluorescence resonance energy transfer (FRET).

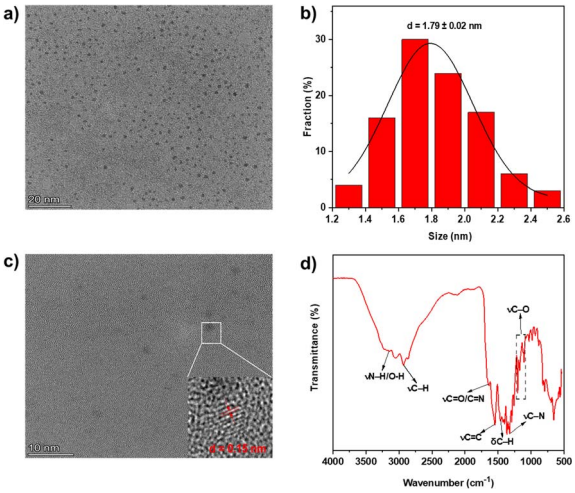

Fig. 1 (a) TEM image of DE-CDs; (b) size distribution histogram of DE-CDs; (c) HRTEM image of DE-CDs; and (d) FTIR spectrum of DE-CDs.

Results and discussion

Synthesis and characterization

Firstly, a series of experiments were conducted to optimize the hydrothermal reaction conditions for DE-CDs. As summarized in Table S1, three typical factors (precursor ratio, reaction temperature and time) were investigated and the optimal conditions for DE-CDs with the highest fluorescence intensity were obtained: L-arginine (0.9 g) and 1-pyrenecarboxaldehyde (0.02 g) in pure water (12.5 mL) at 190 °C for 4 h (Table S1 and entry 2).

Then, the morphological structure and surface functional groups of DE-CDs were characterized. As shown in the transmission electron microscopy (TEM) image, DE-CDs are uniform in size (Fig. 1a) and narrowly distributed with an average particle size of 1.79 nm (Fig. 1b). The high-resolution TEM (HRTEM) image reveals that the DE-CDs have lattice fringes with lattice spacing of 0.15 nm, indicating the graphene structure of DE-CDs (Fig. 1c). From the typical X-ray diffraction (XRD) pattern in Fig. S1, a broad peak at 11° might be caused by the layered structure of carbon material,[19] and a weak peak at around 20° corresponds to the peak of graphite (002).[20] The surface functional groups of DE-CDs were analyzed by Fourier transform infrared spectroscopy (FTIR). As shown in Fig. 1d, the broad absorption peak at 3226 cm^{-1} corresponds to the N–H/O–H bond stretching vibration.[21] Peaks at 2932 and 1468 cm^{-1} are attributed to the stretching and bending vibrations of C–H bonds, respectively.[14b,22] The two peaks at 1640 and 1548 cm^{-1} correspond to the stretching vibrations of the C=O/C=N and C=C bonds, respectively.[14a,22] The peak at 1325 cm^{-1} and the absorption band from 1203 to 1030 cm^{-1} correspond to the stretching vibrations of the C–N and C–O bonds, respectively.[14] These results show the successful synthesis of carbon dots, and the hydrophilic surface groups would be helpful in enhancing the stability and sensing ability of DE-CDs in aqueous solution.

Next, the elemental composition was investigated by X-ray photoelectron spectroscopy (XPS) as shown in Fig. 2. The full-scan XPS spectrum shows three distinct peaks at 284.09, 399.95 and 530.43 eV, indicating the presence of C 1s (65.55%), N 1s (17.13%) and O 1s (17.32%), respectively (Fig. 2a). The high-resolution C 1s spectrum shows three fitted peaks at 283.92, 285.02 and 287.33 eV, corresponding to C–C/C=C, C–O and C=O bonds, respectively (Fig. 2b).[23] On the high-resolution O 1s spectrum (Fig. 2c), two fitted peaks appear

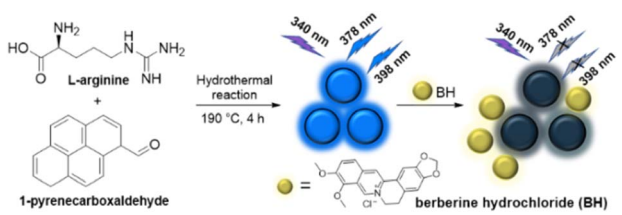

Scheme 1 Synthesis of DE-CDs and the fluorescence detection of BH.

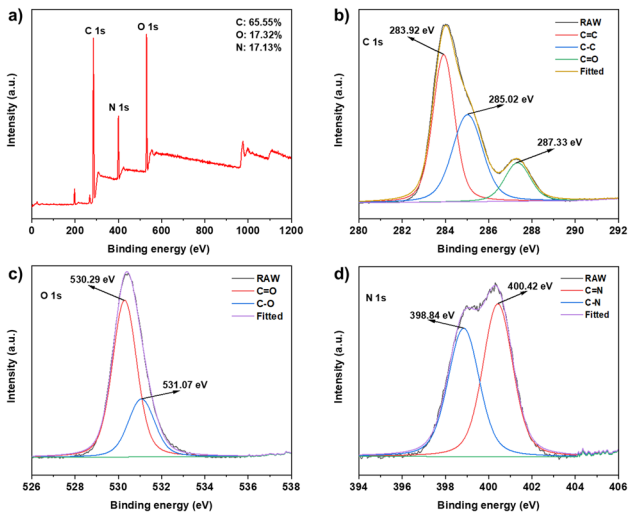

Fig. 2 XPS spectra of DE-CDs: (a) full scan. (b–d) High-resolution spectra of C 1s, O 1s and N 1s.

at 530.29 and 531.07 eV, representing C=O and C–O bonds, respectively.[23] The high-resolution N 1s spectrum (Fig. 2d) shows two peaks at 398.84 and 400.42 eV, indicating the existence of C–N and N–H bonds, respectively.[24,25] All these results are consistent with those of FTIR studies, showing the presence of a large amount of oxygen- and nitrogen-containing groups on DE-CDs and providing the basis for the subsequent fluorescence sensing in aqueous solution.

Optical properties

The optical properties were characterized by UV-vis and fluorescence spectroscopy. As shown in Fig. 3a, the UV-vis absorption spectrum of DE-CDs shows an absorption band at 269 nm, which should be attributed to the π–π* transition of the conjugated C=C bond. Besides, the peak at 334 nm might be caused by the n–π* transition of the C=N/C=O bond.[26,27] The fluorescence spectrum shows that the optimal excitation and emission wavelengths of DE-CDs are 340 and 378/398 nm, respectively. The fluorescence quantum yield (FLQY) of DE-CDs is measured to be 46% using quinine sulfate as reference (Fig. S2). Due to the short absorption wavelength and highly dual-fluorescence emission, the aqueous solution of DE-CDs shows a light-yellow color under sunlight and strong blue fluorescence under 365 nm UV light (inset of Fig. 3a). When the excitation wavelength increases from 280 to 360 nm, the fluorescence emission peaks of DE-CDs are almost unchanged (Fig. 3b). Generally, the excitation-independent emission property indicates uniform particle size and similar surface states of DE-CDs. In addition, the fluorescence intensities under different conditions were recorded to study the stability of DE-CDs (Fig. 3c–f). It can be seen that the two fluorescence emission peaks remain almost unchanged under continuous irradiation at 340 nm for 90 min, incubation temperatures (5–85 °C), pH values (3–12) and NaCl concentrations (0–100 mM). The excellent performance of DE-CDs (photobleaching resistance, thermostability, pH stability and salt tolerance) indicate that DE-CDs could adapt well to its environment and provide a guarantee for its application in fluorescence sensing.

Sensing property

The sensing selectivity of DE-CDs was investigated by adding 16 common ions (Al^{3+}, Ca^{2+}, Cu^{2+}, Fe^{3+}, K^{+}, Mg^{2+}, Na^{+}, Zn^{2+}, Br^{-}, Cl^{-}, CO_3^{2-}, F^{-}, I^{-}, NO_3^{-}, PO_4^{3-} and SO_4^{2-}) and 11 common compounds (glutathione (GSH), glucose, L-glycine (L-Gly), L-arginine (L-Arg), L-glutamic acid (L-Glu), L-histidine (L-His), ascorbic acid (AA), nicotinamide, citric acid (CA), urea and berberine chloride (BH)) to DE-CDs aqueous solutions. As shown in Fig. 4a, the fluorescence intensities of the two emission peaks (378/398 nm) are both more significantly quenched by BH than by other ions and compounds. The anti-interference ability of DE-CDs was also investigated (Fig. S3) and showed that the selectivity of DE-CDs for BH was not affected. The investigation of response time shows that the fluorescence signals of DE-CDs at 378/398 nm were completely quenched by BH at the beginning of the reaction (<10 s) (Fig. S4). In order to investigate the applicability and sensitivity of DE-CDs for sensing BH, the fluorescence intensities of DE-CDs solutions containing different amounts of BH were measured. As shown in Fig. 4b, the fluorescence intensities of DE-CDs gradually

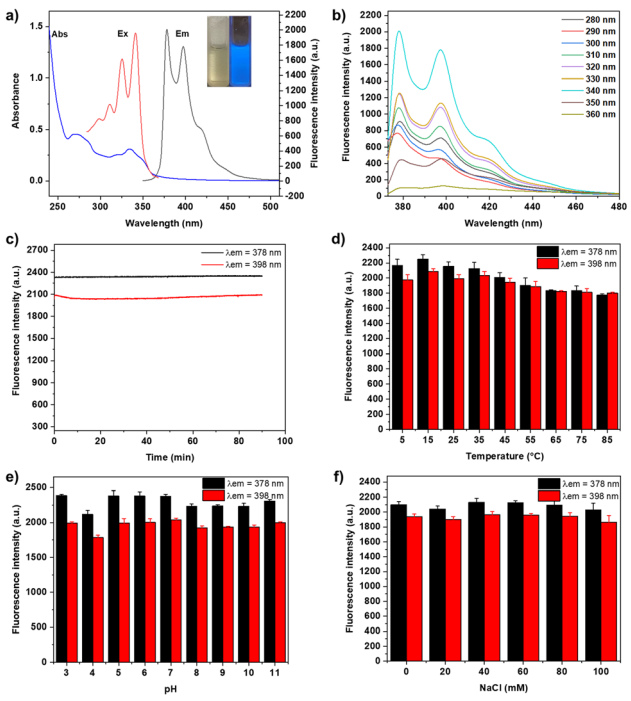

Fig. 3 (a) UV-vis absorption, fluorescence excitation and emission spectra of DE-CDs (insets: photographs of DE-CDs solution under sunlight (left) and 365 nm UV light (right)). (b) Fluorescence emission spectra of DE-CDs excited at different wavelengths. (c–f) Fluorescence intensities of DE-CDs at 378/398 nm (black/red): (c) on continuous excitation at 340 nm and (d–f) at different incubation temperatures, pH and NaCl concentrations ($n = 3$).

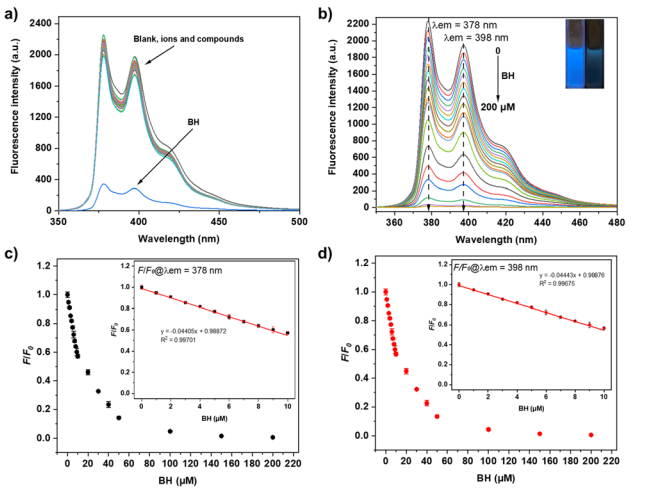

Fig. 4 (a) Fluorescence spectra of DE-CDs with different ions or compounds (BH = 50 μM, other ions or compounds = 100 μM). (b) Fluorescence spectra of DE-CDs at different concentrations of BH (insets: photographs of DE-CDs solutions without (left)/with (right) BH (50 μM) under 365 nm UV light. (c and d) The relationship between F/F_0 and the concentration of BH at (c) 378 and (d) 398 nm.

decreased with increasing amount of BH. Fig. 4c and d display the quenching efficiency F/F_0 at 378 and 398 nm *versus* the BH concentration, where F_0 and F are the fluorescence intensities of DE-CDs solution without and with BH, respectively. The linear equation for the peak at 378 nm was defined as $F/F_0 = -0.0440\ C(\mathrm{BH}) + 0.9888$ with a correlation coefficient of $R^2 = 0.9970$ and that at 398 nm was defined as $F/F_0 = -0.0444\ C(\mathrm{BH}) + 0.9888$ with $R^2 = 0.9967$ over the range of 0–10 μM (insets of Fig. 4c and d). It can be seen that the two peaks showed similar sensitivity to BH in aqueous solution. The limit of detection (LoD) was calculated to be 0.32 and 0.30 μM at 378 and 398 nm, respectively, through the $(3\sigma/k)$ method, where σ is the standard deviation of the blank sample ($n = 10$) (Table S2) and k is the slope of the linear calibration curve. Compared with previously reported works,[14] DE-CDs in this work exhibit a fast and dual response to BH, which indicates that DE-CDs may serve as a more sensitive fluorescence sensor for the rapid quantitative analysis of BH.

Actual sample testing

In order to validate the practical feasibility of the above method, the detection of BH in actual samples was further investigated, and the results calculated through the two linear equations at 378 and 398 nm are shown in Table 1. As can be seen, the recoveries of BH in berberine hydrochloride tablet and capsule were both 92–110% with acceptable relative standard deviations (RSD < 5%). These results make DE-CDs a potential double-guarantee sensor for BH detection in pharmaceutical analysis.

Quenching mechanism

In order to explore the possible quenching mechanism of DE-CDs, a series of experiments were carried out as follows. Firstly, as shown in Fig. 5a, the experimental UV-visible absorption spectra of DE-CDs/BH mixtures were consistent with the theoretical absorption spectra, which rules out the formation of non-fluorescent ground state complexes.[14] Fig. 5b shows that the UV-vis absorption spectrum of BH overlaps with both the excitation and emission spectra of DE-CDs, which suggests the possible presence of the internal filtering effect (IFE) and fluorescence resonance energy transfer (FRET).[18] Three negative zeta potentials of −27.6, −18.0 and −2.6 mV indicate that there was no electrostatic attraction between the DE-CDs and the BH (Fig. 5c). From Fig. 5d, we can see that the fluorescence lifetimes of the DE-CDs changed significantly

Table 1 Detection of BH in actual samples (λ_{em} = 378/398 nm, n = 3)

Sample	Added (μM)	Found (μM)	Recovery (%)	RSD (%)
BH tablet	0	3.43/2.70	—	0.83/0.93
	2	5.86/5.16	108.07/109.68	0.58/0.61
	4	7.97/7.31	107.35/109.07	1.97/1.93
	6	9.26/8.62	98.25/99.00	1.28/1.26
BH capsule	0	2.19/1.84	—	3.39/1.50
	2	4.10/3.98	97.83/103.74	4.53/4.54
	4	5.78/5.66	93.33/96.87	4.62/4.57
	6	7.57/7.42	92.46/94.60	2.00/2.18

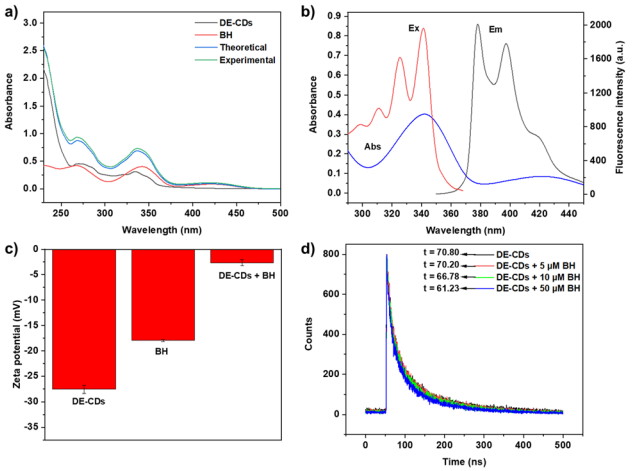

Fig. 5 (a) UV-vis absorption spectra of DE-CDs and BH, theoretical and experimental spectra of DE-CDs/BH. (b) UV-vis absorption spectra of BH, fluorescence excitation and emission spectra of DE-CDs. (c) Zeta potentials of DE-CDs, BH, and DE-CDs/BH (n = 3). (d) Fluorescence lifetimes of DE-CDs without/with BH (λ_{ex} = 340 nm, λ_{em} = 378 nm).

before and after the addition of different concentrations of BH (70.80, 70.20, 66.78 and 61.23 ns), which suggests the existence of FRET.[28] Finally, the occupancy of the IFE was calculated to be 62.66% at 378 nm according to Parker's equation. The static and dynamic quenching mechanisms of DE-CDs were further ruled out by the Stern-Volmer equation (Table S3 and Fig. S6).[29] Therefore, the quenching mechanism of DE-CDs by BH was proposed to be a combination of IFE and FRET.

Conclusions

In summary, blue fluorescent DE-CDs with high fluorescence quantum yield (46%) and dual-emission property were efficiently prepared from L-arginine and 1-pyrenecarboxaldehyde by a one-pot hydrothermal method. Morphological and optical characterization showed the successful synthesis of carbon dots with uniform size, and the as-prepared DE-CDs demonstrated superior photobleaching resistance, thermostability, pH stability and salt tolerance. In addition, the two fluorescence emission peaks could be quenched by BH through a combination mechanism involving IFE (62.66%) and FRET, with good linear correlation in the range of 0–10 μM. Based on this, a fluorescence sensing platform was developed for the detection of BH with high selectivity and sensitivity (LoD = 0.32 and 0.3 μM), short response time (<10 s) and acceptable recoveries and RSD in actual samples. The above outstanding advantages of DE-CDs are expected to make them an alternative double-guarantee sensor for BH detection in the quality evaluation of traditional Chinese medicine and in pharmaceutical analysis.

Author contributions

Yang Geng, Ze-Yue Zhao, Wei Zhang and Long-Teng Li: methodology, formal analysis, investigation and visualization. Ye

Tian, Bai-Qiang Zhai and Wen-Zhu Bi: conceptualization, analysis, and writing – review & editing. Wen-Jie Zhang and Yang-Guang Wang: validation and supervision.

Conflicts of interest

There are no conflicts to declare.

Data availability

The data supporting this article have been included as part of the SI.

Acknowledgements

This work was supported by the Key Scientific Research Project of Colleges and Universities in Henan Province (26A150051), the Key Research Project of Zhengzhou Railway Vocational and Technical College (2025KY005) and the Science and Technology Development Plan Project Henan Province (242102311178).

Notes and references

1 S. Gaba, A. Saini, G. Singh and V. Monga, *Biorg. Med. Chem.*, 2021, **38**, 116143.
2 M. T. Suadoni and I. Atherton, *Complement. Ther. Clin. Pract.*, 2021, **42**, 101287.
3 Z. Ilyas, S. Perna, S. Al-thawadi, T. A. Alalwan, A. Riva, G. Petrangolini, C. Gasparri, V. Infantino, G. Peroni and M. Rondanelli, *Biomed. Pharmacother.*, 2020, **127**, 110137.
4 M. Hashemzaei and R. Rezaee, *Phytother. Res.*, 2021, **35**, 2846.
5 M. Zhou, Y. Deng, M. Liu, L. Liao, X. Dai, C. Guo, X. Zhao, L. He, C. Peng and Y. Li, *Eur. J. Pharmacol.*, 2021, **890**, 173655.
6 Y. Wang, Y. Liu, X. Du, H. Ma and J. Yao, *Cancer Manage. Res.*, 2020, **12**, 695.
7 A. Duda-Madej, P. Lipska, S. Viscardi, H. Bazan and J. Sobieraj, *Cellsl*, 2025, **14**, 1041.
8 J. Wang, Y. Jiang, B. Wang and N. Zhang, *J. Sep. Sci.*, 2019, **42**, 1794.
9 S. Uzaşçı and F. B. Erim, *J. Chromatogr.*, 2014, **1338**, 184.
10 (*a*) A. Geto, M. Pita, A. L. De Lacey, M. Tessema and S. Admassie, *Sens. Actuators, B*, 2013, **183**, 96; (*b*) J. F. Song, Y. Y. He and W. Guo, *J. Pharm. Biomed. Anal.*, 2002, **28**, 355.
11 (*a*) X. He, X. Li, S. Feng, X. Li and C. Nong, *J. Electrochem. Soc.*, 2021, **168**, 056523; (*b*) S. Chen, C. Xu, X. Zhu, Z. Li, H. Bie, Y. Yang, J. Yu, Y. Yang and H. Huang, *Anal. Chim. Acta*, 2024, **1304**, 342579; (*c*) Y. Zhao, H. Zhang, X. Zhou, Y. Zhang, T. Cheng and X. Li, *Sens. Actuators, B*, 2025, **443**, 138262; (*d*) N. A. Alarfaj, S. A. Altamimi, M. F. El-Tohamy and F. M. Al-Suqayhi, *Int. J. Electrochem. Sci.*, 2021, **16**, 210348.
12 (*a*) P. Biparva, S. M. Abedirad, S. Y. Kazemi and M. Shanehsaz, *Sens. Actuators, B*, 2016, **234**, 278; (*b*) R. Tian, J. Chen, D. Li, X. Sun and H. Ma, *Spectrochim. Acta, Part A*, 2024, **305**, 123417; (*c*) J. Xiong, L. Yang, L. X. Gao, P. P. Zhu, Q. Chen and K. J. Tan, *Anal. Bioanal. Chem.*, 2019, **411**, 5963; (*d*) D. X. Chen and Y. F. Long, *J. Fluoresc.*, 2024, DOI: 10.1007/s10895-024-04033-9; (*e*) Z. Hu, M. Xie, D. Yang, D. Chen, J. Jian, H. Li, K. Yuan, Z. Jiang and H. Zhou, *RSC Adv.*, 2017, **7**, 34746; (*f*) S. Liang, Y. Kuang, F. Ma, S. Chen and Y. Long, *Biosensors Bioelectron.*, 2016, **85**, 758.
13 (*a*) F. Yan, S. Li, R. Tong, Y. Wang, Y. Fu and L. Chen, *ACS Appl. Nano Mater.*, 2025, **8**, 3709; (*b*) M. Tuerhong, Y. Xu and X. B. Yin, *Chin. J. Anal. Chem.*, 2017, **45**, 139; (*c*) J. Ren, H. Opoku, S. Tang, L. Edman and J. Wang, *Adv. Sci.*, 2024, **11**, 2405472; (*d*) A. Hebbar, R. Selvaraj, R. Vinayagam, T. Varadavenkatesan, P. S. Kumar, P. A. Duc and G. Rangasamy, *Chemosphere*, 2023, **313**, 137308; (*e*) R. Dhiman, J. Kumar and M. Singh, *Anal. Sci.*, 2024, **40**, 1387.
14 (*a*) F. Yan, Z. Sun, S. Luo and H. Zhang, *Dyes Pigm.*, 2021, **192**, 109446; (*b*) M. Liu, X. Du, K. Xu, B. Yan, Z. Fan, Z. Gao and X. Ren, *J. Anal. Sci. Technol.*, 2021, **12**, 11; (*c*) J. M. Liang, F. Zhang, Y. L. Zhu, X. Y. Deng, X. P. Chen, Q. J. Zhou and K. J. Tan, *Spectrochim. Acta, Part A*, 2022, **275**, 121139.
15 X. Zhu, W. Jiang, Y. Zhao, H. Liu and B. Sun, *Trends Food Sci. Technol.*, 2021, **111**, 388.
16 T. Li, Y. Dong, G. Pang, J. Zhao, G. Wang, Z. Li and Q. Fu, *Diamond Relat. Mater.*, 2025, **152**, 111883.
17 (*a*) Y. Liu, F. Liang, J. Sun, R. Sun, C. Liu, C. Deng and F. Seidi, *Nanomaterials*, 2023, **13**, 2869; (*b*) J. Ma, L. Sun, F. Gao, S. Zhang, Y. Zhang, Y. Wang, Y. Zhang and H. Ma, *Molecules*, 2023, **28**, 8134; (*c*) N. M. Hoang, N. Thi Bich Ngoc, N.-A. Tran, N. X. Ho, H.-L. Thi Dang, D. V. Cuong, V. T. Trang, P. Thi Lan Huong, P. Thi Thanh Huyen, M. S. Jamil, S. Yun, L. T. Tu, L. N. D. Pham and V.-D. Dao, *J. Environ. Chem. Eng.*, 2025, **13**, 117696.
18 (*a*) C. S. Ni, W. J. Zhang, W. Z. Bi, M. X. Wu, S. X. Feng, X. L. Chen and L. B. Qu, *RSC Adv.*, 2024, **14**, 26667; (*b*) Y. Geng, Z. Y. Zhao, W. Zhang, B. Q. Zhai, Y. Tian and W. Z. Bi, *RSC Adv.*, 2025, **15**, 19696.
19 L. Cao, M. Zan, F. Chen, X. Kou, Y. Liu, P. Wang, Q. Mei, Z. Hou, W.-F. Dong and L. Li, *Carbon*, 2022, **194**, 42.
20 M. S. Devi, T. D. Thangadurai, N. Manjubaashini and D. Nataraj, *Diamond Relat. Mater.*, 2023, **136**, 110021.
21 X. Hou, Y. Hu, P. Wang, L. Yang, M. M. Al Awak, Y. Tang, F. K. Twara, H. Qian and Y.-P. Sun, *Carbon*, 2017, **122**, 389.
22 V. Sharma, S. K. Singh and S. M. Mobin, *Nanoscale Adv.*, 2019, **1**, 1290.
23 Y. He, H. Wang, Y. Yan, X. Jiang, H. Zou and Z. Zhang, *Spectrochim. Acta, Part A*, 2024, **310**, 123942.
24 J. Wei, H. Li, Y. Yuan, C. Sun, D. Hao, G. Zheng and R. Wang, *RSC Adv.*, 2018, **8**, 37028.
25 S. Wu, C. Zhou, C. Ma, Y. Yin and C. Sun, *J. Chem.*, 2022, **2022**, 3737646.
26 R. Atchudan, T. N. J. I. Edison, S. Perumal, R. Vinodh, A. K. Sundramoorthy, R. S. Babu and Y. R. Lee, *Chemosensors*, 2021, **9**, 166.
27 Y. Zhao, X. Zhu, L. Liu, Z. Duan, Y. Liu, W. Zhang, J. Cui, Y. Rong and C. Dong, *Nanomaterials*, 2022, **12**, 2377.
28 M. Ganiga and J. Cyriac, *Sens. Actuators, B*, 2016, **225**, 522.
29 M. Lu, C. Pan, X. Qin and M. Wu, *ACS Omega*, 2023, **8**, 14499.